JOURNAL OF OPTOELECTRONICS AND ADVANCED MATERIALS Vol. 8, No. 4, August 2006, p. 1359 - 1366

Influence of deposition temperature on the structural and optical properties of $InSbSe_3$ films

H. E. ATYIA
Physics Department, Faculty of Education, Ain Shams University, Roxi, Cairo, Egypt

Thermal evaporation technique was used to prepare $InSbSe_3$ films on clean glass substrates maintained at various deposition temperature (T_d = 473, 523 and 593 K). X- ray diffraction analysis showed the occurrence of amorphous to polycrystalline transformation in the films deposited at higher substrate temperature $T_d \geq 523$ K. Compositions of these films have been characterized by (EDX) analysis. Transmittance and reflectance measured in the wavelength rang (500-2500 nm), used to calculate the optical constant (refractive index n and absorption index k). The deposition temperature dependent of the optical constants n and k was determined in the spectral range. Analysis of optical absorption data as a function of T_d yields the existence of wide band tails increase in width with increasing deposition temperature and indirect allowed transitions with optical energy gap decreases from 1.13 to 0.92 eV as the deposition temperature T_d increases from 423 to 593 K. The dispersion of the refractive index for films could be described using the Wemple - Di Domenico single oscillator model, change of the dispersion parameters were also studied as a function of deposition temperature. The high frequency dielectric constant. The ratio of the carrier concentration to the effective mass (N/m^*), relaxation time (τ), and dissipation factor ($\tan\delta$) were studied as a function of deposition temperature.

(Received June 19, 2006; accepted July 20, 2006)

Keywords: Deposition temperature, Optical dispersion parameter, Complex dielectric constant

1. Introduction

Chalcogenides glasses has attracted much attention in the field of electronic as well as in infrared optics, since they exhibit several particular phenomena useful for devices such as electrical switches, memories, image storage and photo resistors.

Like other members of the III-VI layered compounds such as Bi_2Se_3 or Sb_2Se_3, and In_2Se_3 compound could be interesting for its semiconducting properties [1-4] because of their importance as a good photovoltaic materials and application in electro-thermal devices [5].

Ternary solid solution is of great technological interest in electronic and photoelectronic devices [6]. The In_2Se_3 - Sb_2Se_3 system has been investigated earlier at least 3 times [7-9] founding finite solid solution of substitution based on the binary compound and an incongruently melting compound with the composition $InSbSe_3$. Some authors studied the physical properties of In-Sb-Se system [10-12]. Few authors studied the optical properties [13] of $InSbSe_3$ single crystals.

The effect of deposition temperature on the optical properties for different semiconductor compounds was studied in a number of papers [14-16].

In the present work a detailed investigation of the structural and optical properties of $InSbSe_3$ films prepared by thermal evaporation method at different deposition temperature above room temperature is carried out.

2. Experimental

$InSbSe_3$ composition was prepared in a bulk form by melting together the stoichiometric amount of the elements In, Sb and Se of purity 99.999% in a sealed evacuated silica tube (10^{-5} Pa) using a oscillatory furnace. The temperature of the furnace was raised to 1223 K by a rate of 50 Kh^{-1} for 48 h [12] then cooled with a rate of 1 K/min^{-1} until room temperature.

Films with different thicknesses were deposited at constant rate by thermal evaporation technique using a coating unit (Edward E 306 A). During the deposition process, the pressure inside the vacuum chamber was maintained at 10^{-5} Torr. The clean glass substrate was mounted on the substrate holder and placed parallel to the material source at a distance of 12 cm. The substrate holder was heated by a insulator heater system and the deposition temperature (T_d) was measured using a thermocouple embedded in the substrate holder underneath the substrates. Films were deposited at T_d ranging from 423 to 593 K. The film thickness was measured using the multiple beam Fizeau fringes method [17].

The chemical composition of films was determined by mean of energy dispersive X- ray spectrometry. An EDX unit attached to a scanning electron microcopy (JOEL 5400) was employed. The structure of the films at different deposition temperature was checked by X- ray diffraction (XRD) analysis (Shimadzu XD-D_2) with Cu target and Ni filter.

The optical transmittance, T, and reflectance, R, of the films were measured at room temperature (295 K) with

unpolarized light at normal incidence in the wave length range (500-2500 nm) using a bauble beam spectrophotometer (JASCO Corp., Model (V-750)).

The optical constants n and k were determined using a computer program (Eureka, the solver). It is based on minimizing $(\Delta R)^2$ and $(\Delta T)^2$, simultaneously, where

$$(\Delta R)^2 = | R(n,k) - R_{exp} |^2$$
$$(\Delta T)^2 = | T(n,k) - T_{exp} |^2$$

The subscript exp and cal refer to the experimental and calculated results respectively, and both the transmittance T and reflectance R are given by using Murmann's exact equations [18,19].

3. Results and discusion

3.1 Structure identification

X-ray diffraction (XRD) patterns obtained for $InSbSe_3$ films deposited on the cleaned glass substrate at different deposition temperatures (T_d) is represented in Fig. 1. It is clear from this figure that films deposited at $T_d \leq 473$ K have an amorphous nature (see Fig. 1 a,b) while the increase of T_d above 473 K films have a polycrystalline nature, and the degree of crystallinty increases with increasing deposition temperature.

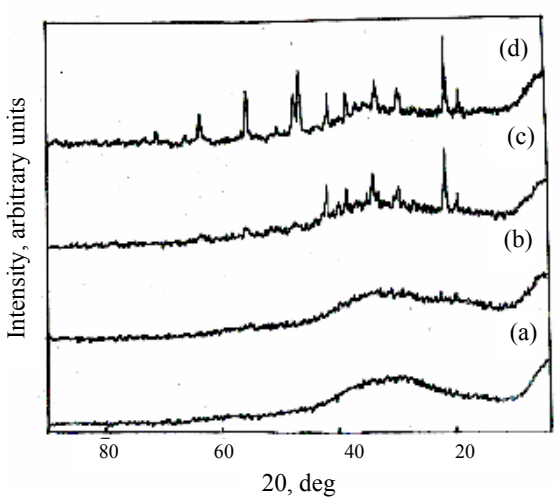

Fig. 1. X-ray diffraction patterns for $InSbSe_3$ films deposited at different deposition temperature T_d (a) T_d =423 K, (b) T_d =473 K, (c) T_d =523 K, (d) T_d =593 K.

A typical energy dispersive X-ray (EDX) spectrum of $InSbSe_3$ films deposited at deposition temperature equal to 523K as a representative example is shown in Fig. 2. This figure is used to found the percentage elemental composition of films, which given in Table 1. The same technique is used for another deposition temperature. This analysis shows that the obtained composition is closed to $InSbSe_3$ within an experimental error ±2% as shown in Table 1.

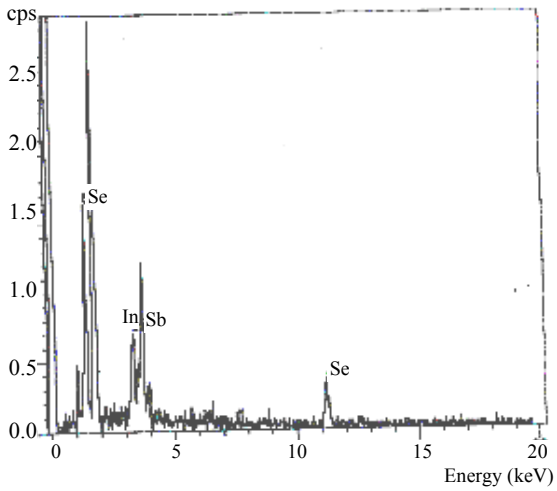

Fig. 2. Energy dispersive X-ray (EDX) spectrum for $InSbSe_3$ films deposited at T_d =523 K.

Table 1. Energy dispersive X-ray data for $InSbSe_3$ films deposited at different deposition temperature.

T_d, K	In%	Sb%	Se%
473	18.76	20.95	60.29
523	20.24	19.17	60.59
593	19.57	20.57	59.86

3.2 Optical properties

3.2.1 Determination of the optical constants

The transmittance T_{exp} and reflectance R_{exp}, of $InSbSe_3$ films deposited at different deposition temperatures, T_d = 473, 523 and 593 K in the thickness range (300-720 nm), were measured in the wavelength range (500 –2500 nm). There has been an increasing need for an accurate knowledge of the optical constants, n and, k, of thin absorbing films over a wide wavelength range, for example in the field of photo thermal conversion of solar cell many new materials have been proposed as constituent of selectively absorbing films.

Taking into account the experimental error in measuring the film thickness to be ±2% and in, T, and, R, to be ±0.5%, the error of the adopted technique in the calculation of the values of, n, and, k, was estimated to be ±1.0% and ±0.5%, respectively. The optical constant, n, and, k, were found to be independent of the film thickness in the investigated range. The spectral distributions of the mean value the refractive index, n, and the absorption index k for $InSbSe_3$ films at different T_d in the studied range ($473 \leq T_d \geq 593$ K) are given in Fig. 3 and 4, respectively.

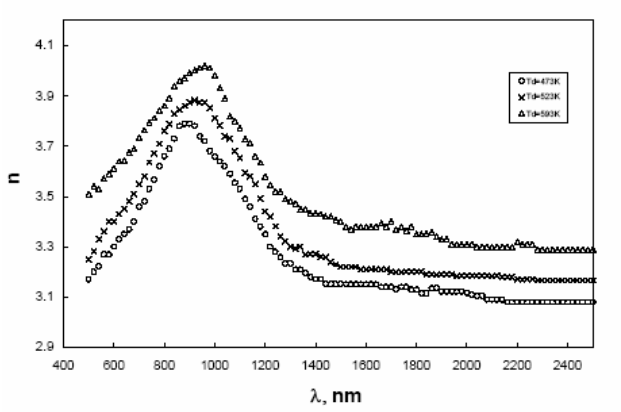

Fig. 3. Dispersion curves of refractive index (n) for $InSbSe_3$ films deposited at T_d = 423, 523 and 593 K.

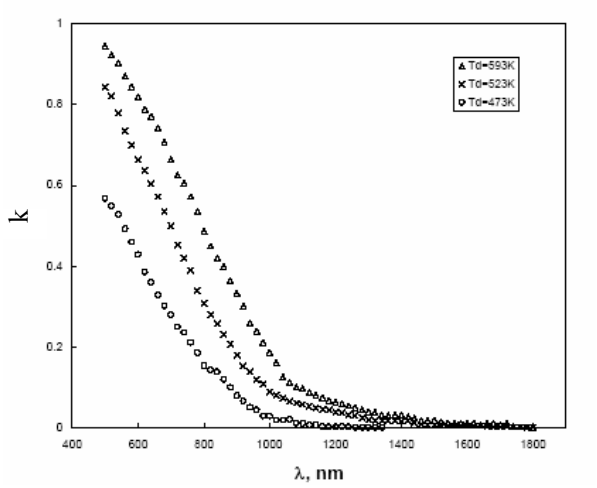

Fig. 4. Dispersion curves of absorption index (k) for $InSbSe_3$ films deposited at T_d = 423, 523 and 593 K.

The dispersion of the refractive index, n, of the amorphous and crystalline $InSbSe_3$ films revealed that the refractive index, n, (at certain λ) increases with increasing deposition temperature. It could be also observed that the refractive index shows anomalous dispersion in the low wavelength range ($500 \leq \lambda \geq 1000$ nm), while for long wavelength ($\lambda > 1000$ nm) n, decreases monotonically, which fact may be attributed to the effect of free carrier concentration, given a peak value at a wavelength λ_c lying in the absorption region ($\lambda < 1000$ nm). This peaks shifted towards longer wavelength with the increase of the deposition temperature of films as shown in Fig. 5.

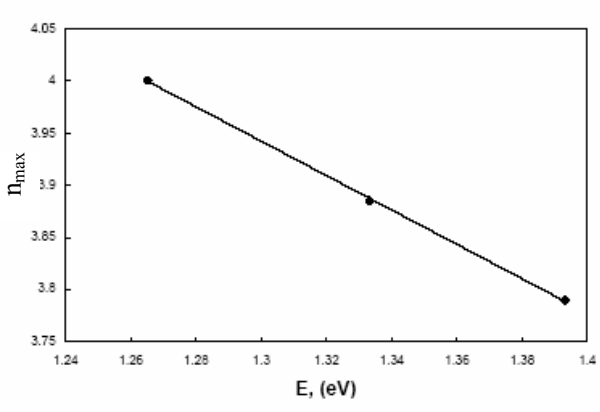

Fig. 5. The maximum refractive index (n max) for$InSbSe_3$ films as a function of photon energy(E).

3.2.2 The spectral distribution of the absorption coefficient (α)

The absorption coefficient α can be calculated using the well – known equation $\alpha = 4\pi k/\lambda$, in which k is substituted by its mean value obtained from Fig. 4.

The absorption coefficient α can be divided into two regions:

1-For absorption coefficient α of less than $\sim 10^{-4}$ cm^{-1} there is usually an Urbach [20] tail where α depends exponentially on the photon energy E, as

$$\alpha = \alpha_o \exp (E / E_e) \quad (1)$$

where α_o is a constant and E_e is interpreted as the width of the tails of localized states in the gap region. To evaluate the values of α_o and E_e, it was α in logarithmic scale as a function of photon energy E as shown in Fig. 6. The values of α_o and E_e for $InSbSe_3$ films at different T_d are tabulated in Table 2. There are evidenced the existence of wide band tails with width that increases with the increase of deposition temperature.

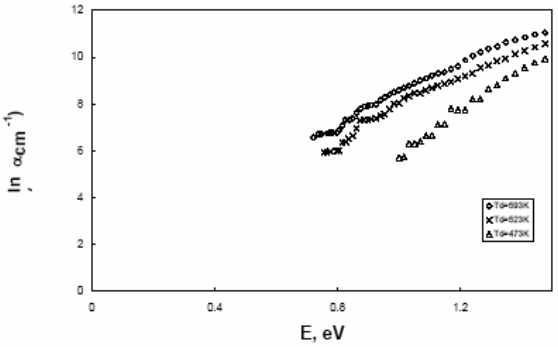

Fig. 6. Plots of ln (α) against photon energy (E) for $InSbSe_3$ films deposited at different T_d.

Table 2. Parameters derived from absorption index (k) for $InSbSe_3$ films deposited at different deposition temperature.

T_d, K	A, $cm^{-1}eV^{-1}$	α_o, cm^{-1}	E_e, eV	E_g^{opt}, eV
473	2.07×10^5	0.00013	0.330	1.13
523	2.5×10^5	0.079	0.347	0.97
593	3.09×10^5	0.158	0.366	0.92

2-For higher values of the absorption coefficient α greater than 10^{-4} cm^{-1}, absorption coefficient takes the form [21,22]:

$$\alpha E = A\,(E - E_g^{opt})^r \qquad (2)$$

where A is the band tailing parameter and is equal to [23]

$$A = (4\pi\sigma/ncE_c) \qquad (3)$$

where c is the speed of light, σ is the minimum metallic conductivity (extrapolated dc conductivity at $T=\infty$), E_c is a measure of the width of the tail states distribution, n is the refractive index, E_g^{opt} is the optical energy gap of the material [24] and r is the power which characterizes the transition process, r = 1/2 for the direct allowed transition, r = 2/3 for the direct forbidden transition, r=2 for the indirect allowed transition and r=3 for the indirect forbidden transition. The study of the spectrum of the absorption coefficient α of a semiconductor in the fundamental region and near the fundamental edge provides us with valuable information about the energy band structure of the material [23].

The usual method for the determination of the value of E_g^{opt} involves plotting a graph of $(\alpha E)^{1/r}$ against E. Fig. 7-a,b show that plots of $(\alpha E)^{1/2} = f(E)$ are linear function and $(\alpha E)^2 = f(E)$ is non linear for $InSbSe_3$ films at different T_d. The linearity indicates the existence of the allowed indirect transitions. Values of a constant A and E_g^{opt} for $InSbSe_3$ films at different deposition temperatures T_d are tabulated in Table 2. It is clear from this Table that E_g^{opt} decreases with increasing T_d. This behaviour is in a good agreement with H. S. Soliman [25] who observed a decrease of E_g^{opt} for $InSbSe_3$ films annealed in air for 1 h at 423 and 473 K.

It has been suggested by many authors [26,27] that in nearly ideal amorphous solids during the process of crystallization, form dangling bonds at the surface of the crystallites. Further more heat treatment (increasing in deposition temperature T_d) causes the crystallites to break down [30] into smaller crystals, thereby increasing the number of surface dangling bonds. These dangling bonds are responsible for the formation of some type of defects in the highly polycrystalline solids. As the number of dangling bonds and defects increases, the concentration of localized states in the band structure also increases, therefore the energy width of the localized state (E_e) and decreases the optical gap (E_g^{opt}) increases.

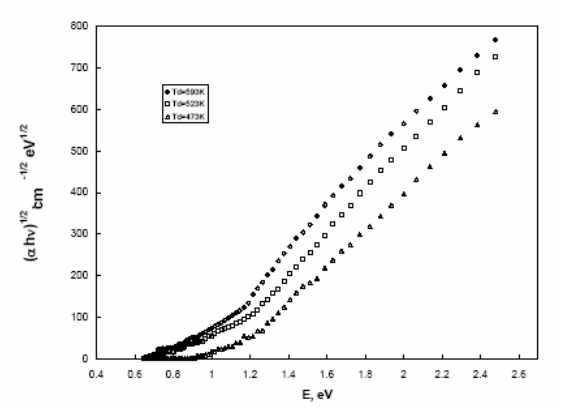

a

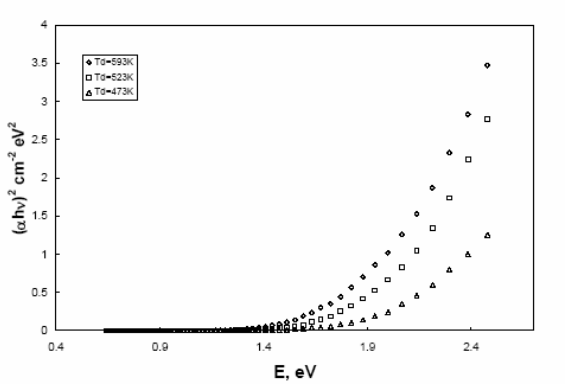

b

Fig. 7-a. Dependence of $(\alpha E)^{1/2}$ as a function of photon energy (E) for $InSbSe_3$ films deposited at different T_d. (b) Dependence of $(\alpha E)^2$ as a function of photon energy (E) for $InSbSe_3$ films deposited at different T_d.

3.2.3 Determination of the dispersion and oscillator energies

The refractive index dispersion data in semiconductors has been analyzed using the concept of the single – oscillator. Within this concept the energy parameters E_d and E_o are introduced and the refractive index, n, at a photon energy E can be expressed by the Wemple and Di Domenicco [28] and Wemple [29] as the following relation

$$(n^2-1) = E_d E_o / (E^2_o - E^2) \qquad (4)$$

The physical meaning of the single – oscillator energy E_o is that it simulates all the electronic excitation involved and E_d is the dispersion energy which related to the average strength of the optical transitions. In practice the dispersion parameters E_d and E_o can be obtained according to equation (4) by a simple plot of $(n^2-1)^{-1}$ versus E^2 as shown in Fig. 8. The values of E_d and E_o can be directly determined from the slope and the intercept on the vertical

axis. The variation of the single – oscillator energy E_o and the dispersion energy E_d with the deposition temperature T_d for $InSbSe_3$ films are shown in Fig. 9 a,b, respectively. It appears that: (i) The oscillator energy E_o decreases slightly with increasing deposition temperature. This can be attributed to the shift of the optical transmission spectra towards the longer wavelength, which corresponds to the shift of the absorption edge towards shorter energy. This can be described as a decrease in the optical gap as a result of an increase of deposition temperature.

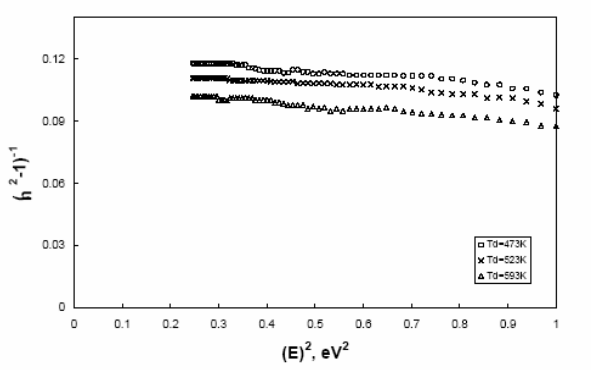

Fig. 8. Plots of $(n^2-1)^{-1}$ against $(E)^2$ for $InSbSe_3$ films deposited at different T_d.

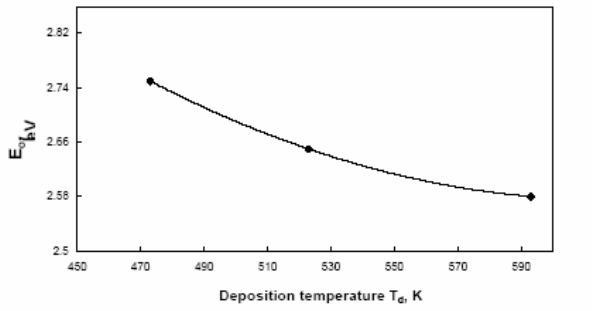

a

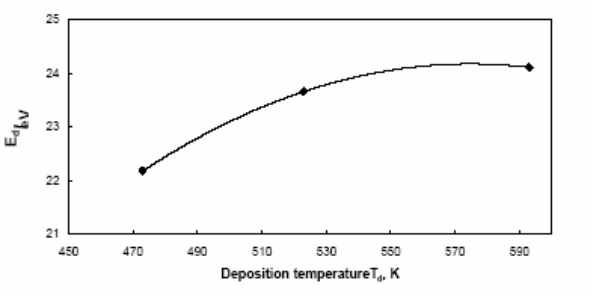

b

Fig. 9-a. Plots of oscillator energy (E_o) versus deposition temperature (T_d) (b) Plots of dispersion energy (E_d) versus deposition temperature (T_d) for $InSbSe_3$ films.

(ii) The dispersion energy E_d increases with increasing deposition temperature. This behaviour can be understoodby considering that obeys, the dispersion energy E_d obyed the simple empirical relation [29]

$$E_d = \beta N_c Z_a N_e \quad (5)$$

where N_c is the number of nearest- neighbor cation to each anion, Z_a is the number of formal chemical valence of the anion, N_e is the total number of valence electron per anion and β is a constant: (0.37 ± 0.05 eV) for covalent compounds and (0.26 ± 0.04 eV) for ionic compounds. As the deposition temperature increases the parameters N_c, Z_a and N_e have the same values while the covalent nature of the structure increases, which corresponds to the increase of β and consequently of the E_d values.

3.2.4 Determination of the high frequency dielectric constant

The data of the refractive index, n, can be analyzed with obtained ε_∞ (high frequency dielectric constant) via two procedures [30]. The first procedure describes the contribution of the free carriers and the lattice vibration modes of the dispersion. The second procedure is based upon the dispersion arising from the bound carriers in an empty lattice.

In the first procedure $\varepsilon_1 = n^2$ can be plotted vs. λ^2 as shown in Fig. 10 for films at different deposition temperatures according to the following relation [30,31]:

$$\varepsilon_1 = n^2 = \varepsilon_\infty - (e^2 N / 4\pi^2 c^2 \varepsilon_o m^*) \lambda^2 \quad (6)$$

where, e, is the electronic charge, ε_o is the vacuum permitivity, N is the charge carrier concentration and m^* is the effective mass. $\varepsilon_{\infty(1)}$ and the ratio N/m^* could be deduced from the intercept and the slope of the straight line in Fig. 10. They are shown in Table 3.

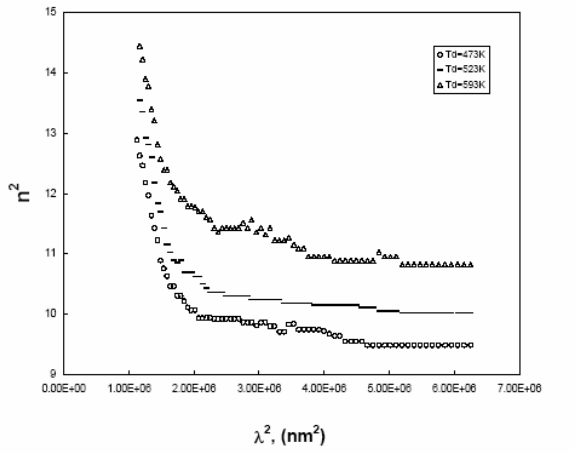

Fig. 10. Plots of (n^2) as a function of λ^2 for $InSbSe_3$ films deposited at different T_d.

Table 3. The parameters derived from refractive index (n) for $InSbSe_3$ films deposited at different deposition temperatures.

T_d, K	$\varepsilon_{\infty(1)}$	λ_o, nm	S_o, m^{-2}	$N/m^* \times 10^{17}$	E_o/S_o,eVm^2	$\varepsilon_{\infty(2)}$
473	9.62	451	3.997×10^{13}	6.82	6.88×10^{-14}	9.33
523	9.90	468	4.08×10^{13}	4.77	6.49×10^{-14}	9.53
593	10.79	480	4.12×10^{13}	3.14	6.27×10^{-14}	10.09

In the second procedure, ε_∞ can be calculated by applying the following simple classical dispersion relation using the single term Sellmeir oscillation [32]

$$\frac{\left(n_\infty^2-1\right)}{n^2-1}=1-\left(\frac{\lambda_o^2}{\lambda^2}\right) \qquad (7)$$

where n_∞ long wavelength refractive index, λ_o the average oscillator wavelength plotting $(n^2-1)^{-1}$ against λ^{-2} as shown in Fig. 11 at different deposition temperatures T_d. Values of λ_o and $\varepsilon_{\infty(2)}$ can be calculated from the linear relation of Fig. 11 for $InSbSe_3$ films as a function of deposition temperature. The values of dielectric constant using the second procedures $\varepsilon_{\infty(2)}$ and λ_o are given in Table 3.

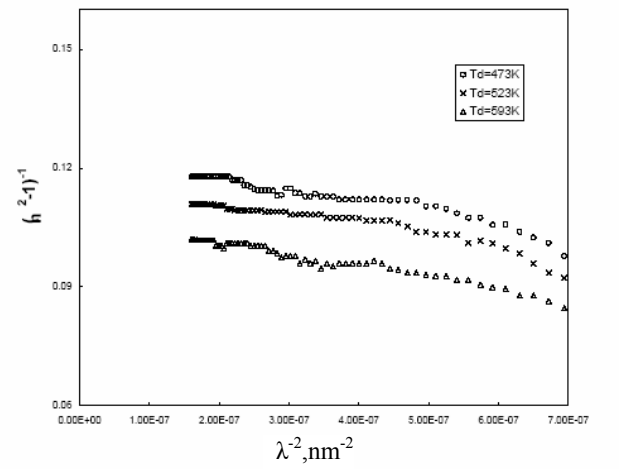

Fig. 11. Plots of $(n^2-1)^{-1}$ against λ^{-2} for $InSbSe_3$ films deposited at different T_d.

It is clear that the values $\varepsilon_{\infty(1)}$ and $\varepsilon_{\infty(2)}$ obtained from the two methods approximately agree with each other, that may be attributed to the lattice vibrations and bounded carriers in an empty lattice. The mean values of the high frequency dielectric constant equals to 9.48, 9.72 and 10.85 for $InSbSe_3$ films deposited at deposition temperature equal to 473, 523 and 593 K, respectively.

The equation (7) can be expressed as [33]

$$n^2-1=(S_o\,\lambda^2{}_o)/(1-(\lambda^2{}_o/\lambda^2)), \qquad (8)$$

where S_o is the average oscillator strength $(S_o=(n^2{}_\infty-1)/\lambda^2{}_o)$. The obtained values of S_o, and E_o/S_o (the refractive index dispersion parameter) for $InSbSe_3$ films as a function of deposited temperatures are given in Table 3. It is clear from this Table that the value of ε_∞ and λ_o increases with increasing T_d and the value of E_o/S_o is of the same order as that obtained by Didomenico and Wemple [34] for a member of materials belonging to several crystal structures: $(6.0\pm0.5)\times10^{-14}$ $eV.m^2$.

3.2.5 Determination of complex dielectric constant

The complex refractive index n=n+ik and the complex dielectric function $\varepsilon^* = \varepsilon_1 + i\varepsilon_2$, where ε_1 and ε_2 are the real and imaginary part of complex dielectric constant ,respectively. ε_1 can be calculated according to equation (6) and the imaginary part ε_2 was determined by the following relation [35]

$$\varepsilon_2=2nk=(\varepsilon_\infty\omega^2{}_p/\,8\pi^2c^3\tau)\lambda^3 \qquad (9)$$

where ω_p is the plasma frequency and τ is the optical relaxation time. The imaginary and real part of dielectric constant can be calculated as it is directly related to the density of states within the forbidden gap of the investigated films [35].

The imaginary and real part of dielectric constant of $InSbSe_3$ films at different deposition temperature T_d are shown in Fig. 12 a,b respectively. One remarks that both ε_1 and ε_2 increase with increasing photon energy as well as increasing deposition temperature.

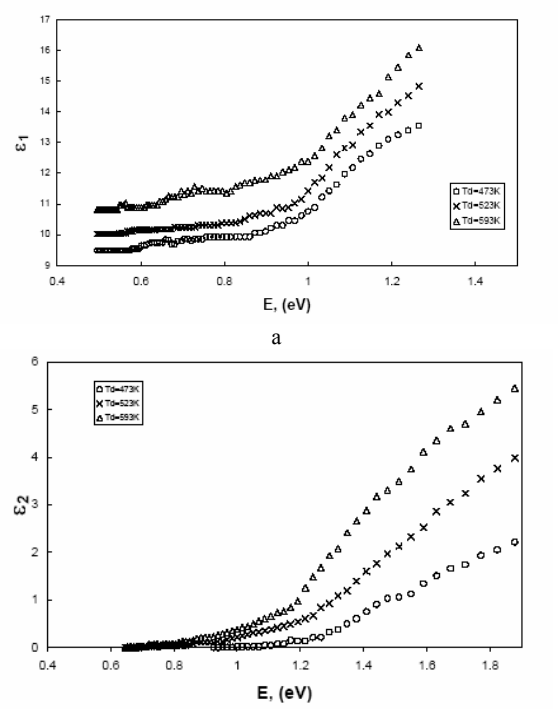

Fig. 12. Plots of dielectric constant ε_1 (a) and dielectric loss ε_2 as a function of photon energy (E) for $InSbSe_3$ films deposited at different T_d.

The dielectric relaxation time can be evaluated by using the following relation [36]:

$$\tau = (\varepsilon_\infty - \varepsilon_1) / \omega\varepsilon_2 \quad (10)$$

Fig. (13) depicts the variation of dielectric relaxation time as a function photon energy for $InSbSe_3$ films at different deposition temperature T_d. This figure shows that the relaxation time increases with increasing photon energy as well as deposition temperature.

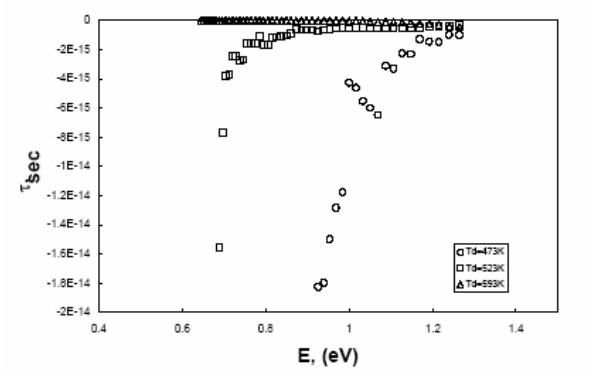

Fig. 13. Dependence of relaxation time (τ) on the photon energy (E) for $InSbSe_3$ films deposited at different T_d.

The dissipation factor tanδ can be calculated according to the relation [37]

$$\tan\delta = \varepsilon_2/\varepsilon_1 \quad (11)$$

The variation of dissipation factor as a function frequency for $InSbSe_3$ films at different deposition temperatures T_d was shown in Fig. 14. This figure shows that the dissipation factor increases with increasing photon energy as well as deposition temperature.

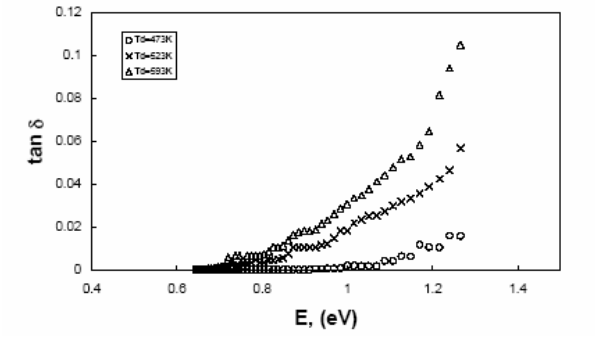

Fig. 14. Dependence of dissipation factor (tan δ) on the photon energy (E) for $InSbSe_3$ films deposited at different T_d.

4. Conclusions

Structural investigation of $InSbSe_3$ films of various thickness, deposited at different deposition temperatures above room temperature shows that the films deposited at temperatures greater than or equal to 523 K have a crystalline structure.

The optical constants n and k of the poly-crystalline and crystalline films are found to be thickness independent over the spectral range. The maximum value of the refractive index n is shifted towards long wavelengths with increasing deposition temperature. The optical transition responsible for optical absorption was indirect one with optical energy gap decreasing with increasing T_d. The dispersion parameters were determined and also studied as a function of the deposition temperature. The values of the real part of the dielectric constant are higher than the imaginary part and both of them increase with increasing photon energy E as well as deposition temperature T_d. The relaxation time τ, and the dissipation factor tan δ, also increase with the deposition temperature.

References

[1] J. Weszka, P. Daniel, A. M. Burian, A. Burian, M. Zelechower, Solid States Commu. (USA). **119**, 533 (2001).
[2] M. A. Afifi, A. E. Bekheet, E. Abd El wahhab, H. E. Atyia, Vacuum **61**, 9 (2001).
[3] I. N. Sahu Thin Solid Films **261**, 98 (1995).
[4] G. Micocci, A. Tepore, R. Rella, P. Siciliano, Phys. Stat. Sol. A **148**, 431 (1995).
[5] C. Julien, M. Eddrif, K. Kambas, M. Balkanski Thin Solid Films **137**, 27 (1986).
[6] M. Lal, P.K. Batham, N. Goyal, Sol. Energy Mater. Sol. Cells **36**, 111 (1995).
[7] D. P. Belotskii, P. F. Babyuk, N. V. Demyanchuk. Low Temperature Thermoelectric Materials, P. 29 Kishinev (1970) (in Russian).
[8] M. Wobst, Z. Metallkd, **58**, 48 (1967).
[9] T. N. Guliev, E. V. Magerramov, P. G. Rustanov, Neorg. Mat. **13**, 627 (1977).
[10] G. Kaur, T. Komatsu, J. Material Sci. (USA) **36**, 4531 (2001).
[11] M. S. Kanboj, G. Kaur, R. Thangaraj, D. K. Avasthi, J. Appl. Phys. (UK) **35**, 477 (2002).
[12] D. Eddike, A. Ramdani, G. Brun, J. C. Tedenac, B. Liautard, Mat. Res. Bull. **33**, 519 (1998).
[13] N. M. Gasanly, B. A. Natiy, A. E. Bakhyshor, K. G. Shirinov, Phys. Stat. Sol. **153**, k89 (1989).
[14] S. Agilan, D. Manjalaraj, Sa. K. Narayandass, G. Mohanrao, Physica B **365**, 93 (2005).
[15] J. J. Valenzuela-Jauregui, R. Ramirez-Bon, A. Mendoza- Galvan, M. Sotelo- Lerma, Thin Solid Films 104 (2003).
[16] C. Viswanathan, V. Senthilkumar,

R. Sriranjini, D. Mangalaraj, Sa. K. Narayandass, Junsin Yi, Crys. Res. Tech. **40**, 658 (2004).
[17] S. Tolansky, in: In Multiple- Beam Interference Microscopy of Metals, Academic, London, 1970, p. 55.
[18] O. S. Heavens, Optical Properties of Thin Solid Films, Dover, New York, 1965.
[19] O. S. Heavens, Thin Films Physics, Methuen, London, 1970.
[20] J. Tauc, Amorphous and Liquid Semiconductors, J. Tauc (Ed), Plenum Press, New York, 1974, P. 159.
[21] J. Tauc, R. Grigorovici, A. Vancu, Phys. Stat. Sol. **15**, 627 (1966).
[22] E. A. Davis, N. F. Mott, Phil. Mag. **22**, 903 (1970).
[23] P. Sharma, M. Vashistha, I. P. Jain, J. Optoelectron. Adv. Mater. **7**, 2647 (2005).
[24] K. L. Bhatia, S. Fabian, S. Kalbitzer, Ch. Klalt, W. Kratschmcr, R. Stall, J.F.P. Sllschop, Thin Solid Films **324**, 11 (1998).
[25] H. S. Soliman, B. A. Khalifa, M. M. El-Nahass, E. M. Ibrahim, Physica B **351**, 11 (2004).
[26] S. Hasegawa, M. Kitagawa, Solid State Commun. **27**, 855 (1978).
[27] S. Hasegawa, S. Yazaki, Solid State Commu. **23**, 41 (1977).
[28] S. H. Wemple, M. Didomenico, Phys. Rev. B **3**, 1338 (1971).
[29] S. H. Wemple, Phys. Rev B **7**, 3767 (1973).
[30] J. N. Zemel, J. D. Jensen, R. B. Schoolar, Phys. Rev. A **140**, 330 (1965).
[31] W. G. Spitzer, N. Y. Fan, Phys. Rev. **106**, 882 (1957).
[32] A. K. Wolaton, T. S. Moss, Proc. R. Soc. **81**, 5091 (1963).
[33] P. A. Lee, G. Said, R. Davis, T. H. Lim, J. Phys. Chem. Solids **30**, 2719 (1969).
[34] M. Didomenico, S. H. Wemple, J. Appl. Phys. **40**, 720 (1969).
[35] A. El-Korashy, H. El-Zahed, M. Radwan, Physica B **334**, 75 (2003).
[36] M. Y. Han, H. Huahy, C. H. Chew, L. M. Gan, X. J. Zhang, W. Ji, J. Phys. Chem. B **102**, 1884 (1998).
[37] F. Vakuphanoglu, A. Cukurovali, I. Yilmaz, Physica B **351**, 53 (2004).

*Corresponding author: hebaelghrip@hotmail.com